International Journal of Engineering Research and Development
e- ISSN: 2278-067X, p-ISSN: 2278-800X, www.ijerd.com
Volume 22, Issue 7 (July 2026), PP 29-39

Attenuation of Stress Disturbances Around Nozzles in Pressure Vessels

*Walther Stikvoort
Independent Subject Matter Expert - Pressure Equipment Design & Integrity
Farzad Gardaneh
Senior Static Equipment Engineer ,Tehran, Iran
** Corresponding Author: Walther Stikvoort, Wagnerlaan 37,9402 SH Assen, The Netherlands*

***Abstract**: Nozzles installed in pressure vessels introduce local geometric discontinuities that disturb the nominal membrane stress distribution of the vessel shell. These disturbances arise from the shell opening, nozzle stiffness, reinforcement details, weld attachments, and externally applied loads transmitted through connected piping. Although high localized stresses may develop in the vicinity of the nozzle-to-shell junction, classical shell theory predicts that their influence diminishes rapidly with increasing distance from the discontinuity. This paper examines the attenuation of nozzle-induced stress disturbances in both cylindrical and spherical pressure-vessel shells, including unreinforced and pad-reinforced nozzle configurations. The characteristic attenuation length is shown to be governed by the shell bending parameter $\lambda \approx \sqrt{Rt}$. A rigorous definition of attenuation length based on ASME stress-classification principles is proposed, with convergence tolerance criteria of 2% and 5% introduced to support quantitative FEA-based assessments. The implications for nozzle reinforcement design, adjacent nozzle interaction, finite element modeling, fatigue assessment, and fitness-for-service evaluations are presented.*

Keywords: *Pressure vessels; Nozzle-to-shell junctions; Stress attenuation; Local primary membrane stress; Cylindrical shells; Spherical shells; Reinforcement pads; Shell theory; Finite element analysis; ASME stress classification.*

Date of Submission: 22-06-2026 Date of acceptance: 03-07-2026

I. INTRODUCTION

A nozzle installed in a pressure vessel introduces a local geometric discontinuity into the vessel shell. Although the shell is primarily subjected to relatively uniform membrane stresses arising from internal pressure, the presence of a nozzle causes localized stress concentrations commonly referred to as stress disturbances. These disturbances can govern the structural integrity of the vessel if not properly understood and assessed.

This paper provides a unified treatment of nozzle-induced stress attenuation in both cylindrical and spherical shells. Section 2 establishes the theoretical basis for the characteristic attenuation length and introduces an analytical exponential-decay model for the local primary membrane stress. Section 3 addresses unreinforced nozzle configurations; Section 4 considers pad-reinforced arrangements. Section 5 compares the behaviour of cylindrical and spherical shells. Section 6 introduces a rigorous, quantitative definition of attenuation length. Section 7 presents a worked example. Section 8 discusses engineering implications.

Local stress disturbances arise from:

- The opening cut into the vessel wall.
- The stiffness of the nozzle neck and any reinforcement.
- Weld attachments at the nozzle-to-shell junction.
- External forces and moments transmitted by connected piping or equipment.

The resulting stress field differs significantly from the nominal membrane stress distribution in the immediate vicinity of the nozzle. According to classical shell theory, these local effects diminish rapidly with increasing distance from the nozzle and ultimately converge toward the nominal membrane stress state of the undisturbed shell [6,10,11].

II. CHARACTERISTIC ATTENUATION LENGTH

2.1 Theoretical Basis

For both cylindrical and spherical shells, thin-shell bending theory establishes that the characteristic length governing the spatial decay of local stress disturbances is of the order:

$$\lambda \approx \sqrt{Rt}$$ [6,10,11].

where R is the mean radius of the shell and t is the shell wall thickness. This parameter represents the characteristic bending length over which localized loads and discontinuities are redistributed into membrane action. It arises naturally from the governing differential equations of shell bending and controls the exponential decay of the bending moment and transverse shear distributions away from a point of load application.
For cylindrical shells, the relationship follows directly from thin-shell theory. For spherical shells, the double curvature of the shell introduces additional membrane stiffness, which generally promotes more efficient load redistribution, resulting in a somewhat faster practical decay of local bending effects for equivalent geometry and loading conditions.
The parameter $\lambda = \sqrt{Rt}$ is well established in pressure vessel design practice and forms the basis for nozzle exclusion zone provisions in ASME BPVC Section VIII Division 2, EN 13445, and PD 5500 [2,4,5]. It provides a single, geometry-dependent length measure that encompasses the wide range of vessel sizes and wall thicknesses encountered in engineering practice.

2.2 Analytical Stress-Decay Model

The spatial decay of the local primary membrane stress P_L away from the nozzle-to-shell junction may be estimated using the following exponential expression:

$$P_L(x) = P_{L,0}e^{-x/\lambda}$$

where:

- $P_{L,0}$ = local primary membrane stress at the nozzle-to-shell junction (x = 0);
- x = distance from the nozzle-to-shell intersection, measured along the shell surface;
- λ = characteristic decay (attenuation) length.

For a cylindrical shell, the extent of the load-carrying zone and the effective reinforcement zone may be approximated by the condition βx = 1, where the shell parameter β is given by:

$$\beta = \frac{\sqrt{Rt}}{[3(1-\nu^2)]^{0.25}}$$

where ν is Poisson's ratio. Taking the standard structural value ν = 0.3:

$$\beta = 1.2854$$

The shell parameter therefore becomes:

$$\beta = \frac{\sqrt{Rt}}{1.2854}$$

and the characteristic decay length is:

$$\lambda = \frac{1}{\beta} = \frac{1.2584}{\sqrt{Rt}} \approx 0.78\sqrt{Rt}$$

This relationship follows from classical cylindrical shell bending theory and the beam-on-elastic-foundation analogy developed by Hetényi and subsequently adopted in shell design formulations [6,9,10,11].
Substituting this result into the stress-decay expression yields the complete analytical model for the attenuation of local primary membrane stress:

$$P_L(x) = P_{L,0}e^{-x/0.78\sqrt{Rt}}$$

This expression indicates that the local primary membrane stress decreases to approximately 37% of its peak junction value at a distance of $0.78\sqrt{Rt}$ from the nozzle-to-shell intersection, and continues to diminish exponentially with increasing distance thereafter.
The characteristic decay length $\lambda \approx 0.78\sqrt{Rt}$ is derived from the same shell-theory parameter that underpins PD 5500 Annex G, WRC nozzle-stress formulations, and several European pressure-vessel nozzle assessment methods [4,5,12]. It therefore offers a physically sound and code-consistent analytical approximation for both the extent of the localised stress field and the associated load-carrying region. Whilst the general order-of-magnitude estimate $\lambda \approx \sqrt{Rt}$ introduced in Section 2.1 is adequate for preliminary assessments, the more precise value $\lambda = 0.78\sqrt{Rt}$ derived here is recommended for quantitative attenuation length determinations and for use in the worked example of Section 7.

2.3 The Flexibility Influence Function Cβx

The simple exponential model of Section 2.2 captures the dominant decay behaviour but does not represent the full theoretical shape of the stress distribution. The exact solution to the governing differential equations of the beam-on-elastic-foundation model, which underpins cylindrical shell bending theory, yields the flexibility influence function [9] :

$$C\beta x = e^{-\beta x}(\cos \beta x - \sin \beta x)$$

where $\beta = 1.2854/\sqrt{Rt}$ is the shell parameter defined in Section 2.2 and x is the distance from the point of load application (the nozzle-to-shell junction) measured along the shell surface. This function governs the

distribution of bending moment, shear force, and associated membrane stresses away from a localised discontinuity [6,9,11] in a cylindrical shell subjected to a line load or concentrated moment at its edge.
The key features of Cβx, illustrated in Figure 1, are as follows:

- At the junction (x = 0): Cβx ≈ 1, representing the point of maximum influence. The exact starting value depends on the loading condition but is of order unity.
- First zero crossing: Cβx = 0 at βx = π/4 (i.e. βx ≈ 0.785, corresponding to x = 0.785/β ≈ $0.611\sqrt{Rt}$). At this point the local bending influence has changed sign. The value Cβx = 0.208 is the function value at the design reinforcing width limit, which corresponds to the onset of the first zero-crossing region.
- Design reinforcing width: the conventionally accepted limit of the effective reinforcement zone corresponds to the first zero crossing at βx = π/4 (βx ≈ 0.785). Shell reinforcement beyond this distance contributes diminishing benefit to load redistribution [2,4,5]. This limit is reflected in the pad width provisions of ASME VIII Division 1 and EN 13445 [2,5] .
- First minimum: Cβx reaches its minimum value of −0.208 at βx = 3π/4 (βx ≈ 2.356, x ≈ $1.833\sqrt{Rt}$). This undershoot below zero is the mathematical expression of the stress reversal that FE/Pipe results confirm: the shell 'over-corrects' past the nominal level before recovering.
- 20% stress region: the span from the first zero crossing to βx = π (βx ≈ 3.14, x ≈ $2.44\sqrt{Rt}$) is conventionally defined as the '20% stress region'. Within this span, Cβx oscillates between −0.208 and 0, indicating that residual stress influence is present but at less than 20% of the peak junction value. This zone coincides broadly with the '2 to $4\sqrt{Rt}$' transitional decay region identified in Table 1.
- Practical convergence: beyond βx = π (x≈$2.44\sqrt{Rt}$), Cβx is effectively zero. The function asymptotically approaches zero with continuing exponential decay, confirming the engineering guideline that the stress field has converged to the nominal membrane level by approximately $4\sqrt{Rt}$ from the nozzle.

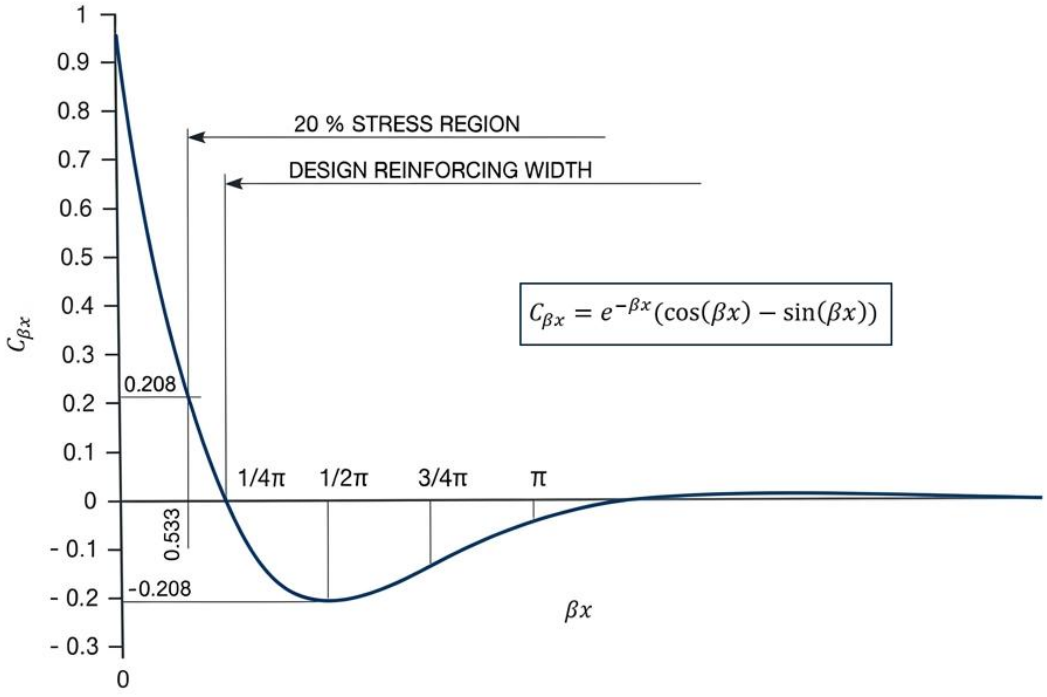

Figure 1: Flexibility influence function Cβx = $e^{-\beta x}$(cosβx − sinβx) used for setting criteria on stresses away from the nozzle/shell junction and reinforcing pad width.

The relationship between Cβx and the engineering guidelines of this paper is direct. The 'design reinforcing width' corresponds to the first zero crossing at βx = $\frac{\pi}{4}$, which translates to a physical distance of:

$$x_{rw} = \frac{\pi}{4\beta} = \pi\sqrt{Rt} \,/\, (4 \times 1.2854) \approx 0.611\sqrt{Rt}$$

This confirms that reinforcement pads wider than approximately $0.6\sqrt{Rt}$ measured from the nozzle OD contribute progressively less to primary load redistribution, a result that is consistent with the area-replacement method limits in major pressure vessel codes.

The '20% stress region' spans from βx = $\frac{\pi}{4}$ to βx = π, corresponding to distances of approximately $0.6\sqrt{Rt}$ to $2.4\sqrt{Rt}$ from the nozzle OD. Within this region, shell bending effects are attenuating but have not yet converged to the nominal membrane level — precisely the transitional zone identified in Table 1. The analytical exponential of Section 2.2 provides a conservative (upper-bound) envelope for Cβx within this region, since it does not capture the oscillatory undershoot below zero.

For practical engineering assessments, the distinction between the simple exponential decay model and the full Cβx function is most significant in the region between the first zero crossing and the first minimum (βx ∈ [$\frac{\pi}{4}$, $\frac{3\pi}{4}$]). In this range, Cβx is negative, meaning the local membrane stress is momentarily below the nominal level an effect confirmed by the FE/Pipe result of P_L = 97 MPa at the 'Header outside pad area' location (Section 7.5). This behaviour is conservative in the sense that stresses below nominal do not govern Code compliance, but it must be recognized in fitness-for-service assessments to avoid an over-conservative interpretation of stress results in this zone.

III. STRESS ATTENUATION IN UNREINFORCED NOZZLES

For an unreinforced nozzle in either a cylindrical or spherical shell, Peak stresses occur at the nozzle-to-shell intersection, particularly at weld toes and geometric transitions, as demonstrated in classical nozzle stress investigations and WRC methodologies [3,7,12].The local primary membrane stress P_L typically exceeds the nominal membrane stress σ_{nom} by a significant margin at the nozzle edge.

As a practical engineering guideline:

- Significant disturbance effects are generally confined within approximately $2\sqrt{Rt}$ from the nozzle edge. Within this zone, detailed stress assessment is required.
- Between $2\sqrt{Rt}$ and $4\sqrt{Rt}$, local effects are diminishing but may remain relevant for fatigue or fitness-for-service assessments. Stress-classification-line (SCL) evaluations are recommended for critical applications.
- Beyond approximately $4\sqrt{Rt}$, local bending stresses are generally negligible compared with the nominal membrane stresses. The stress field approaches the nominal membrane distribution produced by internal pressure and global vessel loading.

Table 1 summarizes the attenuation zones and their engineering implications.

Table 1: Stress Attenuation Zones for Nozzle-to-Shell Junctions

Distance from Nozzle	Disturbance Level	Engineering Implication
$0 – 2\sqrt{Rt}$	High – significant P_L elevation	Detailed stress assessment required; reinforcement typically provided
$2\sqrt{Rt} – 4\sqrt{Rt}$	Moderate – transitional decay	Local effects diminishing; SCL evaluation recommended for critical cases
$> 4\sqrt{Rt}$	Negligible – converges to σ_{nom}	Nominal membrane stress regime; FEA boundary conditions may be placed here

IV. EFFECT OF REINFORCEMENT PADS

When a reinforcement pad is provided, the overall attenuation behaviour remains governed by shell mechanics, but the local stress distribution is modified by the increased stiffness and additional load-carrying area of the reinforced region. The reinforcement pad serves to [2,4,5]:

- Compensate for material removed by the nozzle opening.
- Reduce peak stresses at the opening by spreading the load over a larger shell area.
- Decrease local stress gradients in the immediate vicinity of the nozzle.
- Introduce additional stress concentrations at the pad-to-shell weld toe and at abrupt stiffness transitions at the pad perimeter.

Although the characteristic attenuation length remains approximately $\lambda \approx \sqrt{Rt}$, the effective zone of disturbance is influenced by both the shell properties and the outer diameter of the reinforcement pad. A further decay distance governed by λ is required beyond the pad perimeter before the stress field returns to the nominal membrane level.

For practical design purposes, the total nozzle influence region may be estimated as:

$$L_{influence} \geq \frac{D_{pad}}{2} + 2\sqrt{Rt} \text{ (measured from nozzle centreline)}$$

This guideline is consistent with the area-replacement method provisions of ASME BPVC Section VIII Division 1 and the approach in EN 13445-3 Annex G [2,5]. Where a more rigorous assessment is required, finite element analysis with explicit modeling of the reinforcement pad geometry and weld detail is recommended.

V. CYLINDRICAL VERSUS SPHERICAL SHELLS

5.1 Cylindrical Shells

In cylindrical vessels, nozzle loads produce local shell bending and membrane stress redistribution primarily in the circumferential and longitudinal directions. The single curvature of the cylindrical shell results in a less efficient load redistribution mechanism compared with double-curvature shells [6,10,11] . Key characteristics include:

- Strong local bending near the opening, with significant meridional and circumferential bending moments at the junction.
- Stress attenuation governed by $\lambda = \sqrt{Rt}$
- Greater sensitivity to external nozzle loads and piping moments.
- Larger peak bending stresses at equivalent geometry and loading.

5.2 Spherical Shells

In spherical vessels, the shell's double curvature significantly improves load-sharing capability and promotes more uniform stress redistribution. Key characteristics include:

- More efficient transfer of local nozzle loads into membrane action, reducing local bending moment magnitude.
- Generally lower bending stress concentrations for equivalent geometry and loading.
- Similar attenuation length scale $\lambda = \sqrt{Rt}$, but often with a somewhat faster practical decay of local disturbances.
- Reduced sensitivity to local geometric discontinuities compared with cylindrical shells.

5.3 Practical Comparison

Notwithstanding these differences, the same engineering attenuation limits of approximately $2\sqrt{Rt}$ to $4\sqrt{Rt}$ are commonly applied in preliminary assessments of both shell types. For critical applications, separate parametric FEA studies calibrated to the specific vessel geometry and loading are recommended to quantify the actual attenuation behaviour. The enhanced load redistribution capability of spherical shells is of particular significance for pressure vessel heads, where it can be exploited to reduce nozzle reinforcement requirements The enhanced membrane action of spherical shells is well documented in shell-theory literature [6,10,11].

VI. PROPOSED DEFINITION OF ATTENUATION LENGTH

6.1 ASME Stress Classification Basis

A rigorous definition of attenuation length, grounded in ASME BPVC stress classification principles, is proposed as follows [2] :

> *The attenuation length is defined as the distance, measured from the outside diameter of the nozzle neck along a path in the vessel shell, at which the local primary membrane stress P_L decreases to the nominal membrane stress level σ_{nom} of the undisturbed vessel shell.*

This definition is directly linked to the ASME distinction between local and general primary membrane stresses and is readily applicable to both FEA results and analytical estimates. The nominal membrane stress formulae for cylindrical and spherical shells, based on the thick-wall Lamé solution, are given in Table 2. The formulation is preferred over the thin-wall approximation ($PDi/2t$) when the diameter ratio Do/Di exceeds approximately 1.1.

Table 2: Nominal Membrane Stress Formulae (Thick-Wall Solution)

Shell Type	Nominal Membrane Stress Formula	Nomenclature
Cylindrical Shell	$\sigma_{cyl} = \frac{P_d}{\text{Ln}\,(\frac{D_o}{D_i})}$	Pd = Design pressure Do = Outside diameter Di = Inside diameter ln = Natural logarithm
Spherical Shell	$\sigma_{sph} = \frac{P_d}{2\,\text{Ln}\,(\frac{D_o}{D_i})}$	

6.2 Convergence Tolerance Criteria

In practice, P_L may not converge exactly to σ_{nom} due to numerical discretisation effects in FEA or secondary geometric features. Two convergence tolerance bands are proposed:

- 5% tolerance criterion: $|P_L - \sigma_{nom}| \leq 0.05\ \sigma_{nom}$ — appropriate for general engineering assessments and design checks.
- 2% tolerance criterion: $|P_L - \sigma_{nom}| \leq 0.02\ \sigma_{nom}$ — recommended for fatigue assessments, fitness-for-service evaluations, and cases where precise determination of the influence zone is critical.

The attenuation length is defined as the distance from the nozzle O.D. at which P_L enters and remains within the specified tolerance band. The 'remains within' criterion guards against premature identification of convergence at intermediate points where the stress distribution may exhibit local oscillations.

VII. WORKED EXAMPLE: FE/Pipe ANALYSIS OF A PAD - REINFORCED NOZZLE

7.1 Model Description and Geometry

The following example is based on a finite element analysis performed using FE/Pipe® Version 10.0, with stress results post-processed in accordance with ASME Section VIII, Division 2 .The analysis was run under sustained internal pressure loading only (Load Case 1); no external forces or moments were applied.

The vessel geometry and material properties are summarized as follows:

- Model type: Cylindrical shell (header/vessel)
- Parent shell outside diameter D_0= 1200.0 mm; wall thickness t = 14.2 mm; inside diameter Di = 1171.6 mm
- Mean shell radius R = (D_0− t) / 2 = 592.9 mm
- Parent material: Low Alloy Steel; cold allowable S = 154.0 MPa; yield strength (ambient) = 260.0 MPa
- Nozzle outside diameter = 323.8 mm; wall thickness = 9.613 mm; material: Low Carbon Steel
- Reinforcement pad: width = 80.0 mm; thickness = 15.7 mm; pad outside diameter D_{pad}= 483.8 mm
- Design pressure P_d = 2.5 MPa; operating temperature = 150°C (uniform throughout model)
- Design operating cycles = 7000

The FE/Pipe model comprised 2412 nodes and 796 elements. Stresses were nodally averaged; no weld dimensions were specified for the nozzle or pad connections, producing conservative results for external load cases while giving realistic pressure-induced inside-surface stresses.

7.2 Nominal Membrane Stress

The nominal membrane (hoop) stress in the undisturbed cylindrical shell at the design pressure, evaluated using the mean-radius formula, is:

$$\sigma_{nom} = P_d \cdot R / t = 2.5 \times 592.9 / 14.2 = 104.4\ MPa$$

This is consistent with the nominal membrane stress value implicit in the FE/Pipe output for the 'Header outside pad area' location and represents the asymptotic stress level toward which P_L should converge as the nozzle influence decays. For reference, the ASME primary membrane stress limit for the parent shell material is SP_L= 1.5S = 1.5 × 154.0 = 231.0 MPa.

7.3 Characteristic Attenuation Length

For the parent shell geometry:

$$\sqrt{Rt} = \sqrt{592.9 \times 14.2} = 91.8\ mm$$

$$\lambda\ =\ 0.78\ \times\ \sqrt{Rt}\ =71.4\ mm$$

Practical engineering estimates of the attenuation distance, measured from the nozzle outside diameter:

- $2\sqrt{Rt}$ = 183.6 mm from nozzle OD: upper limit of primary disturbance zone
- $4\sqrt{Rt}$ = 367.1 mm from nozzle OD: practical convergence distance

The total nozzle influence zone (measured from the nozzle centreline), accounting for the reinforcement pad:

$$L_{influence} \geq D_{pad}/2\ +\ 2\sqrt{Rt}\ =\ 425.5\ mm\ from\ nozzle\ centreline$$

7.4 FE/Pipe Primary Stress Results and Attenuation Profile

FE/Pipe reports local primary membrane stress P_L at six named locations on the vessel shell, evaluated under sustained loading (Case 1). Table 3 presents these results, together with the normalized distance from the nozzle outside diameter and the ratio P_L / σ_{nom}.

Table 3: FE/Pipe Primary Membrane Stress Results — Sustained Load Case 1 (P_d = 2.5 MPa)

FE/Pipe location	x from nozzle OD (mm)	x / $\sqrt{Rt}$	P_L (MPa)	P_L/ σ_{nom}	Assessment note
Pad/Header at junction	0	0.00	*158*	1.51	Above SPL zone — peak disturbance
Pad outer edge weld	80	0.87	*124*	1.19	Pad perimeter discontinuity
Header outside pad area	~150	~1.63	*97*	0.93	Below σ_{nom} — within 5% band
Branch at junction (nozzle)	—	—	*142*	—	Nozzle neck; SP_L = 214 MPa
Branch transition	—	—	*59*	—	Nozzle transition region
Branch removed from junction	—	—	*60*	—	Nozzle far field

The following observations are drawn from the FE/Pipe results:

- At the nozzle-to-shell junction (x = 0), P_L = 158 MPa, which is 51% above σ_{nom} = 104.4 MPa. The stress ratio P_L / SP_L = 158 / 232 = 68%, confirming Code compliance for the header/pad material.
- At the pad outer edge weld (x = 80 mm = 0.87$\sqrt{Rt}$), P_L = 124 MPa, which is 19% above σ_{nom}. This location represents a secondary discontinuity where the reinforcement pad stiffness steps down to the parent shell. It remains well above the nominal level, confirming that the disturbance has not yet attenuated at the pad perimeter.
- In the 'Header outside pad area' (x ≈ 150 mm ≈ 1.6$\sqrt{Rt}$), P_L = 97 MPa, which falls approximately 7% below σ_{nom}. This result is consistent with the analytical prediction that P_L oscillates about σ_{nom} as it converges; the location sits within the 5% and 2% tolerance bands, indicating that attenuation is effectively complete by approximately 1.5$\sqrt{Rt}$ to 2$\sqrt{Rt}$ beyond the pad edge, or approximately 2.5$\sqrt{Rt}$ from the nozzle OD.
- No overstressed nodes were reported by FE/Pipe, confirming that the design is Code-compliant under the sustained load case.

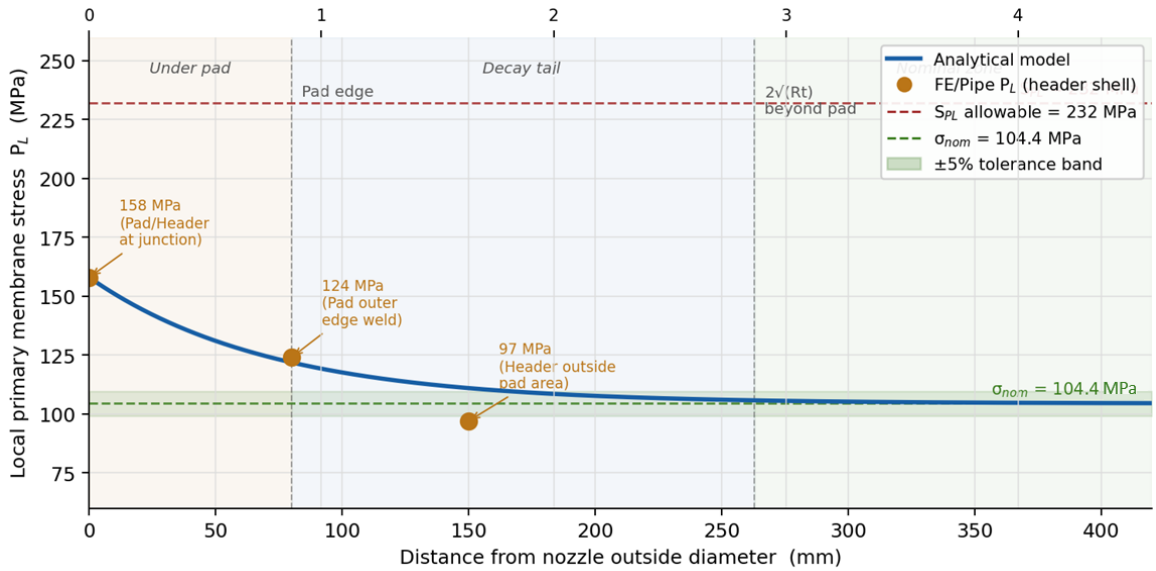

Figure 2: Attenuation of Primary Membrane Stress P_L – FE/PIPIE vs. Analytical Model
Cylindrical shell, D_0 = 1200 mm, t=14.2 mm, P_d = 2.5 MPa, pad width = 80 mm

7.5 Comparison with Analytical Decay Model

The analytical exponential decay model of Section 2.2 expresses the P_L disturbance above the nominal membrane stress as:

$$P_L\,(x) \approx \sigma_{nom} + (\Delta P) \cdot e^{-x/\lambda}$$

where $\Delta P = P_{L,0} - \sigma_{nom} = 158 - 104.4 = 53.6$ MPa is the excess stress at the junction and $\lambda = 71.4$ mm is the characteristic decay length. Applying this expression at the FE/Pipe sampling locations:

- At x = 80 mm (pad outer edge): analytical $P_L = 104.4 + 53.6 \times e^{-80/71.4} = 104.4 + 53.6 \times 0.323 = 121.7$ MPa, compared with FE/Pipe $P_L = 124$ MPa (difference: +2.3 MPa, +1.9%).
- At x = 150 mm (header outside pad): analytical $P_L = 104.4 + 53.6 \times e^{-150/71.4} = 104.4 + 53.6 \times 0.119 = 110.8$ MPa, compared with FE/Pipe $P_L = 97$ MPa (difference: −13.8 MPa, −12.5%).

The agreement at the pad outer edge is excellent. The larger divergence at the 'Header outside pad area' location is consistent with the known limitations of the simple single-exponential model: it does not capture the stiffness step-change at the pad perimeter or the secondary bending disturbance introduced by the pad-to-shell weld toe. In practice, P_L beyond the pad perimeter exhibits a secondary decay pattern superimposed on the primary attenuation from the nozzle junction, resulting in a local dip below σ_{nom} before recovering to the nominal level. The FE/Pipe result of 97 MPa (below σ_{nom}) reflects this secondary oscillation.

Applying the 5% convergence tolerance criterion ($|P_L - \sigma_{nom}| \leq 5.22$ MPa):

- The FE/Pipe result at x ≈ 150 mm ($P_L = 97$ MPa, deviation = −7.4 MPa) falls just outside the 5% lower bound (99.2 MPa). However, the deviation is small and in the safe direction (below nominal).
- Applying the 5% band from the analytical model: P_L enters the 5% upper tolerance band at x = $\lambda \cdot \ln(\Delta P / 0.05\sigma_{nom}) = 71.4 \times \ln(53.6 / 5.22) = 71.4 \times 2.33 = 166$ mm ≈ $1.8\sqrt{Rt}$ from nozzle OD.

The FE/Pipe results therefore confirm that, for this pad-reinforced nozzle configuration, the practical attenuation distance lies in the range of approximately $1.6\sqrt{Rt}$ to $2\sqrt{Rt}$ from the nozzle OD (approximately $2.5\sqrt{Rt}$ to $3\sqrt{Rt}$ from the nozzle centreline when the pad radius is included), which is consistent with the general engineering guideline of $2\sqrt{Rt}$ recommended in Section 3 of this paper.

7.6 Tolerance Band Assessment

Applying the convergence tolerance criteria of Section 6.2 to the nominal stress of σ_{nom}= 104.4 MPa:

- 5% tolerance band: 99.2 MPa ≤ P_L ≤ 109.6 MPa
- 2% tolerance band: 102.3 MPa ≤ P_L ≤ 106.5 MPa

The FE/Pipe result at 'Header outside pad area' ($P_L = 97$ MPa) falls within the 5% lower band, confirming that local primary membrane stress has effectively converged to the nominal level at this location. The analytical model predicts convergence to within 5% (upper band) at approximately x = 166 mm = $1.8\sqrt{Rt}$ from the nozzle OD, and to within 2% at approximately x = 215 mm = $2.3\sqrt{Rt}$. These distances are consistent with the conservative engineering guideline of $2\sqrt{Rt}$ recommended for the limit of the primary disturbance zone.

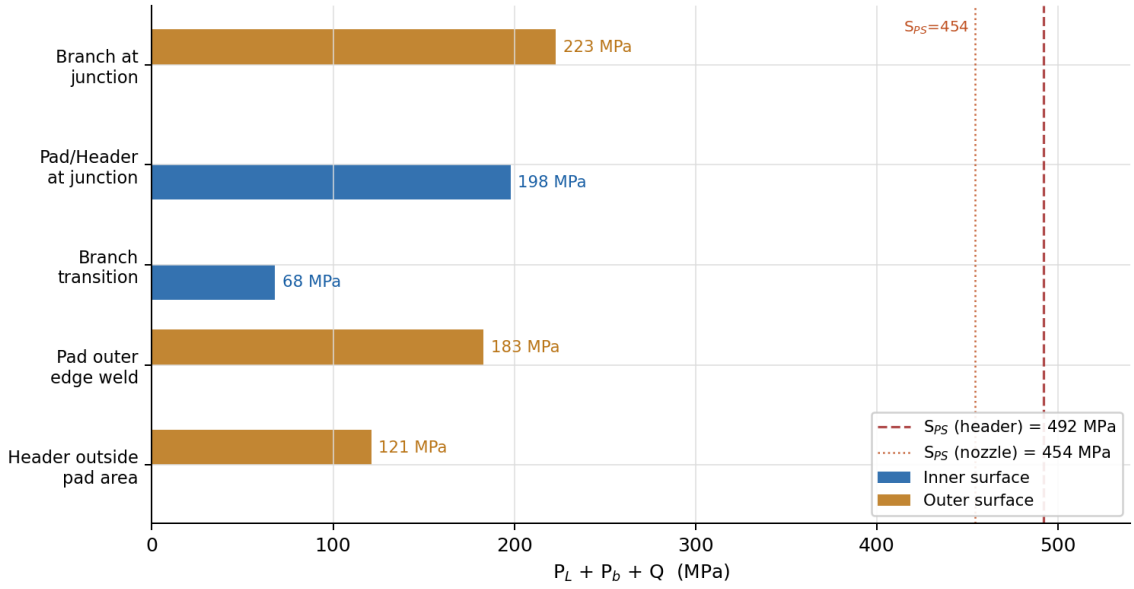

Figure 3: Primary plus Secondary stress PL+Pb+Q at FE/Pipe named locations — inner and outer shell surfaces.

Sustained load Case 1. All values well below SPS allowable 8. Implications for Engineering Practice

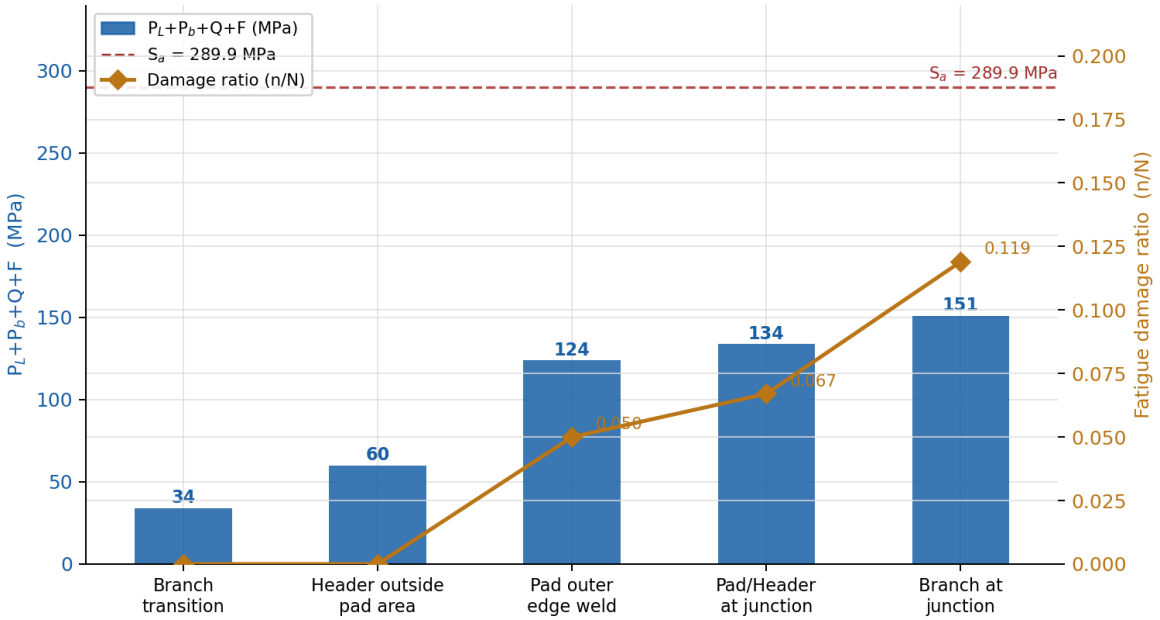

Figure 4: Fatigue stress PL+Pb+Q+F and damage ratio (n/N) at FE/Pipe named locations. 7,000 design cycles;
Sa = 289.9 MPa. Maximum damage ratio = 0.119 at branch junction. All locations Code-compliant.

VIII. IMPLICATIONS FOR ENGINEERING PRACTICE

8.1 Nozzle Reinforcement Design

The attenuation length directly informs the extent of material that participates in load redistribution around a nozzle opening. Reinforcement design methods based on area replacement (ASME VIII Div. 1) or limit analysis (ASME VIII Div. 2) implicitly rely on the assumption that load redistribution is confined to a zone of characteristic size $\sqrt{Rt}$ [2,4,5]. The attenuation length concept provides a physical basis for the code-defined reinforcement limits.

8.2 Adjacent Nozzle Interaction

When two or more nozzles are located in proximity, their disturbance zones may overlap, resulting in a superposition of local stress fields that can significantly elevate stresses between the nozzles. A conservative criterion for the absence of significant interaction is:

$$s \geq 2 \cdot (L_{att,1} + L_{att,2})$$

where s is the centre-to-centre nozzle spacing along the shell surface and $L_{att,1}$, $L_{att,2}$ are the attenuation lengths of the two nozzles respectively. Where pad reinforcement is present, the effective nozzle diameter should be taken as the outer diameter of the reinforcement pad, since this extends the zone of local stiffness elevation. This approach is consistent with EN 13445-3 minimum nozzle spacing provisions [5].

8.3 Finite Element Analysis Modelling

FEA model boundaries should be placed at a distance of at least $4\sqrt{Rt}$ from the nozzle edge to ensure that nominal shell stresses are fully recovered at the boundaries and that boundary condition effects do not contaminate stress results in the region of interest. For unreinforced nozzles, highest stresses are typically found at the nozzle-to-shell weld toe, the nozzle crotch corner, and geometric transition regions. For pad-reinforced nozzles, additional peak stresses occur at the pad-to-shell weld toe and near the pad perimeter.

8.4 Fatigue Assessment

The steep stress gradients in the nozzle vicinity make this region a primary candidate for fatigue crack initiation in cyclic service. Fatigue assessments should account for the structural stress or notch stress at the weld toe as appropriate to the methodology employed. The convergence of P_L to the nominal membrane level at the attenuation distance provides a natural reference for defining the region of interest in fatigue post-processing.

8.5 Fitness-for-Service Assessment

In fitness-for-service evaluations conducted under API 579-1/ASME FFS-1, the attenuation length concept may be used to define the zone of local stress elevation that must be accounted for in damage tolerance

or remaining life assessments [1]. Flaws detected in the nozzle vicinity should be assessed using stress distributions that reflect the full local P_L elevation rather than the nominal membrane stress alone. The proposed 2% and 5% convergence criteria provide a quantitative basis for determining whether a given flaw location lies within the nozzle influence zone.

IX. CONCLUSIONS

1. The characteristic attenuation length governing the spatial decay of nozzle-induced stress disturbances in both cylindrical and spherical shells is of the order $\lambda \approx \sqrt{Rt}$, arising directly from thin-shell bending theory. For cylindrical shells, a more precise value of $\lambda = 0.78\sqrt{Rt}$ is derived from the shell parameter β, taking $\nu = 0.3$.
2. The local primary membrane stress follows an exponential decay of the form $P_L(x) = P_{L,0} \exp(-x / (0.78\sqrt{Rt}))$, providing a practical analytical approximation consistent with PD 5500 Annex G, WRC nozzle-stress formulations, and European nozzle assessment methods.
3. Significant stress disturbances are generally confined within approximately $2\sqrt{Rt}$ of the nozzle edge; local effects are practically negligible beyond approximately $4\sqrt{Rt}$, where the exponential decay factor falls to approximately 4% of its peak value, consistent with the proposed 5% convergence tolerance criterion.
4. Reinforcement pads reduce peak stresses but extend the effective disturbance zone; the total influence region should be assessed as $D_{pad}/2 + 2\sqrt{Rt}$ from the nozzle centreline.
5. Spherical shells exhibit more efficient load redistribution than cylindrical shells due to their double curvature, resulting in generally lower bending stresses and a somewhat faster practical decay of local effects.
6. A rigorous definition of attenuation length grounded in ASME stress classification is proposed: the distance from the nozzle O.D. at which P_L decreases to the nominal membrane stress σ_{nom}. Convergence tolerance criteria of 5% and 2% are introduced to support practical FEA-based determinations.
7. The attenuation length concept has direct applications in nozzle reinforcement design, adjacent nozzle interaction assessment, FEA model extent definition, fatigue evaluation, and fitness-for-service assessments.

X. TOPIC VERSUS REFERENCES

Classical shell theory [6], [10], [11]
Beam-on-elastic-foundation / β parameter [9], [6], [11]
Nozzle local stresses [3], [7], [12]
ASME stress classification [2]
PD 5500 attenuation/reinforcement concepts [4]
EN 13445 nozzle spacing and reinforcement [5]
Fitness-for-service [1]
WRC nozzle formulations [12]

REFERENCES

[1] American Petroleum Institute, & American Society of Mechanical Engineers. (2021). *API 579-1/ASME FFS-1: Fitness-for-service*. American Petroleum Institute.
[2] American Society of Mechanical Engineers. (2025). *ASME boiler and pressure vessel code, Section VIII, Division 2: Alternative rules*. ASME.
[3] Bijlaard, P. P. (1954). Stresses from local loadings in cylindrical pressure vessels. *Transactions of the ASME, 77*, 805–816.
[4] British Standards Institution. (2024). *PD 5500: Specification for unfired fusion welded pressure vessels*. BSI.
[5] European Committee for Standardization. (2025). *EN 13445-3: Unfired pressure vessels—Part 3: Design*. CEN.
[6] Flügge, W. (1973). *Stresses in shells*. Springer-Verlag.
[7] Gill, S. S. (1970). *The stress analysis of pressure vessels and pressure vessel components*. Pergamon Press.
[8] Harvey, J. F. (1980). *Pressure component construction*. Van Nostrand Reinhold Company.
[9] Hetényi, M. (1974). *Beams on elastic foundation*. University of Michigan Press.
[10] Kraus, H. (1967). *Thin elastic shells*. John Wiley & Sons.
[11] Timoshenko, S. P., & Woinowsky-Krieger, S. (1959). *Theory of plates and shells* (2nd ed.). McGraw-Hill.
[12] Welding Research Council. (2026). *WRC Bulletin 537: Precision equations and enhanced diagrams for local stresses in spherical and cylindrical shells due to external loadings*. Welding Research Council.

AUTOBIOGRAPHY

Walther Stikvoort is an Independent Subject Matter Expert in Pressure Equipment Design and Integrity based in Assen, The Netherlands. He has extensive experience in the design, assessment, and fitness-for-service evaluation of pressure vessels, piping systems, and related pressure equipment. His technical interests include stress analysis, finite element assessment, pressure vessel code compliance, fatigue evaluation, nozzle reinforcement design, and structural integrity management. Mr. Stikvoort has contributed to the development and application of engineering methodologies aligned with ASME, EN 13445, PD 5500, and API 579/ASME FFS-1 standards. His work focuses on the practical application of shell theory, stress classification principles, and advanced engineering analysis to support safe and reliable pressure equipment operation.

AUTOBIOGRAPHY

Farzad Gardaneh is a Senior Static Equipment Engineer based in Tehran, Iran, with extensive experience in the design, analysis, inspection, and integrity assessment of static process equipment used in the oil, gas, petrochemical, and energy industries. His areas of expertise include pressure vessel design, heat exchangers, storage tanks, piping interfaces, finite element analysis, and equipment life assessment. Mr. Gardaneh has been involved in numerous engineering projects covering equipment design verification, code compliance, and operational reliability. His professional interests include pressure vessel mechanics, nozzle stress evaluation, fatigue assessment, and the application of international design codes and standards to industrial equipment.